JPSE (Journal of Physical Science and Engineering), Vol. 7, No. 1, 2022, Page 16–22.
DOI: 10.17977/um024v7i12022p016

JPSE
(Journal of Physical Science and Engineering)

http://journal2.um.ac.id/index.php/jpse
EISSN: 2541-2485

Study of the Structure of $Mn_xFe_{3-x}O_4$-Poly(*m*-Aminobenzene Sulfonic Acid) Composites Based on Natural Sand

Received
27 January 2022

Revised
30 March 2022

Accepted for Publication
08 April 2022

Published
15 April 2022

A Choerullah[1], S Sunaryono[1,2]*, A Hidayat[1], and N A N N Malek[3]

1. Department of Physics, Faculty of Mathematics and Natural Sciences, Universitas Negeri Malang, Jl. Semarang 5, Malang, 65145, Indonesia.
2. PUI-PT Center of Advanced Materials for Renewable Energy (CAMRY), Universitas Negeri Malang, Jl. Semarang 5, Malang, 65145, Indonesia.
3. Department of Biosciences, Faculty of Science, Universiti Teknologi Malaysia, Skudai, Johor, 81310, Malaysia.

***E-mail:** sunaryono.fmipa@um.ac.id

Abstract

$Mn_xFe_{3-x}O_4$-Poly(*m*-ABS) nanocomposite has been successfully synthesized by *in-situ* polymerization. In the formation of $Mn_xFe_{3-x}O_4$-Poly(*m*-ABS) nanocomposites, FeCl synthesized from iron sand acts as an oxidant and *m*-aminobenzenesulfonic acid (*m*-ABS) as a monomer. Structural characterization has been successfully carried out using XRD, FTIR, and SEM. XRD test results show that the $Mn_xFe_{3-x}O_4$-Poly(*m*-ABS) nanocomposite has a particle size of about 10.62 nm. The appearance of peaks (111) and (620) with low intensity indicated the presence of poly(*m*-ABS). This low intensity was probably caused by the amorphous character of polyaniline and its derivatives. The FTIR results show the appearance of asymmetrical and symmetrical S=O strains, S-O, and C-S strains are the main characteristics of poly(*m*-ABS) which indicate the success of monomer polymerization. The results of the SEM test show that circular shapes dominate the particles with varying sizes with an average size of 42 nm. This result is different from the XRD results because SEM can only measure the surface of the particles, so the resulting size tends to be larger. Based on the study of the structure obtained shows that the $Mn_xFe_{3-x}O_4$-Poly(*m*-ABS) nanocomposite has the potential to be applied to energy conversion devices.

Keywords: $Mn_xFe_{3-x}O_4$, poly(*m*-aminobenzenesulfonic acid), structure, nanoparticles.

1. Introduction

The development of nanotechnology currently has a strategic role in various industrial products, including telecommunications, pharmacy and medical, cosmetics, textiles, electronic devices, optoelectronics, and energy conversion devices [1]. The role of nanotechnology, especially in energy conversion, is currently an exciting research area to study and explore. One that is being studied a lot is magnetite nanoparticles. Magnetite (Fe_3O_4) has a wide application. Magnetic is a group of ferrimagnetic materials in their bulk size. At the nanometer size, magnetic becomes a superparamagnetic material with promising properties such as biocompatibility and environmental stability [2]. Magnetite can also transduce external magnetic field energy into thermal and mechanical responses used in biomedical applications [3]. However, to obtain good performance from magnetite, functionalization is needed. This functionalization is carried out by coating the magnetite surface with both organic and inorganic polymers [4].

In recent years researchers have focused on synthesizing nano-polymer composites with magnetite particles because of their flexibility for applications in engineering. The polymer that is the centre of research at this time is conductive. One of the most popular conductive polymers is polyaniline. Polyaniline has become a concern because it has unique properties, *i.e.* good environmental stability, high electrical conductivity, and low cost [5]. Wang *et al.* [6] reported that Fe_3O_4/Polyaniline has the potential for supercapacitors. Its ferromagnetic behaviour indicates this with a 4.22–48.4 emu/g saturation magnetization and increased thermal stability. Sadegh *et al.* [7] reported that Fe_3O_4@PANI plays a role in increasing solar cell efficiency. Its superparamagnetic properties indicate with saturation magnetization of 44.09 emu/g and Power Conversion Efficiency (PCE) of 1.53%. Sunaryono *et al.* [8]

reported that magnetite composites with polyaniline can also be applied as drug delivery media in cancer therapy. In their study [8], Mn doping was also reported to obtain good magnetic properties with optimal saturation magnetization values. However, the polyline has poor solubility in water or organic solvents. Based on that problem, substituted polyaniline was developed, especially sulfonated polyaniline, which can increase the solubility and ability of polyaniline [9]–[12]. This magnetite composite and its derivatives from polyaniline have been reported by Modarresi-Alam *et al.* [11] for the synthesis process using the solid-state method. Then Shabzendedar *et al.* [12] reported that magnetite composites with *m*-aminobenzenesulfonic acid (NCPABS-Fe_3O_4) could be applied as solar cell polymers. This is evidenced by the PCE of 4.24%. However, studies on magnetite doped with Mn and composited with polyaniline derivatives have not been widely reported. Therefore, it is necessary to conduct a study on $Mn_xFe_{3-x}O_4$-Poly(*m*-ABS) nanocomposites.

In this study, we report the successful synthesis of natural sand-based $Mn_xFe_{3-x}O_4$-Poly(*m*-ABS) nanocomposite using *in-situ* polymerization. In this study, *m*-ABS was used as a monomer and FeCl from natural sand, which acts as an oxidant in the polymerization process and as a precursor in forming Fe_3O_4 as a source of Fe^{2+} and Fe^{3+}. The addition of Mn doping is expected to maximize the role of magnetite to obtain an increase in magnetic properties [13]. This study aimed to examine the structure formed from the $Mn_xFe_{3-x}O_4$-Poly(*m*-ABS) nanocomposite. For this reason, X-Ray Diffractometer (XRD) characterization was carried out to determine the formed sample phase and ensure the synthesis's success. Then the Fourier Transform Infrared (FTIR) characterization was used to analyze the functional groups formed from the composite and Scanning Electron Microscope (SEM) to determine the surface morphology and particle size of the $Mn_xFe_{3-x}O_4$-Poly(*m*-ABS) composite.

2. Method

2.1. Material

The materials used in this study include, *i.e.* iron sand from Sine beach Tulungagung (Indonesia), hydrochloric acid 37%, *m*-aminobenzenesulfonic acid, $MnCl_2.4H_2O$ 99.9%, ammonia solution (NH_4OH) 25%, and aquades.

2.2. Synthesis of $Mn_xFe_{3-x}O_4$-Poly(m-ABS)

The iron sand is separated first by using a permanent magnet until the sand is free from impurities. The pure iron sand powder was weighed as much as 20 grams, reacted with 58 mL HCl for 30 minutes with a hotplate magnetic stirrer, and then filtered to produce FeCl. Then 18 mL of filtered FeCl was mixed with $MnCl_2$ and stirred for 30 minutes until homogeneous. After the mixture was homogeneous, 7 mmol (1.2124 g) *m*-ABS was added in two stages with a distance of 10 minutes. Stirring was continued for up to 1 hour until the colour of the mixture changed to brown. Then the mixture was left at 40–45 °C for 24 hours, after which it was cooled at room temperature. The mixture was then reacted with 25 mL of NH_4OH and stirred with a hotplate magnetic stirrer for 30 minutes. After the mixing process is complete, the mixture is washed with distilled water and filtered with filter paper. The final stage is the residual solids obtained in the oven at a temperature of 100 °C for 1 hour until a blackish-brown powder is obtained.

3. Result and Discussion

3.1. FTIR Characterization

The results of the FTIR spectrum of the $Mn_xFe_{3-x}O_4$-Poly(*m*-ABS) nanocomposite can be seen in Figure 1. The wide absorption at 3,588 cm^{-1} is defined as the O-H strain, representing water in the $Mn_xFe_{3-x}O_4$-Poly(*m*-ABS) nanocomposite. The stretching pattern corresponds to the O-H absorption in the value range 3,750–3,000 cm^{-1} [14], [15]. The peaks of 1,643 cm^{-1} and 1,601 cm^{-1} showed absorption bands indicated as stretches of C=N and C=C quinoids [10], [16]–[18], then peaks of 1,483 cm^{-1} and 1,414 cm^{-1} were identified as benzenoid [17], [19]–[22]. The absorption peak of 1,314 cm^{-1} is represented as an aromatic C-N strain band [7], [9], [11], [12]. The absorption bands at 1,267 cm^{-1} were identified as O=S=O asymmetric strains, and the absorption peaks of 1,111 cm^{-1} and 1,040 cm^{-1} were allocated as O=S=O symmetric stretches [9], [11], [23]. The strong absorption peak at 1,207 cm^{-1} is represented as a $C\text{-}N^{\cdot+}$ vibration which shows the characteristic polaron shape, which is a specific band in protonated and doped conductive polymers [7], [12], [19]–[22]. Absorption at 620 cm^{-1} and 725 cm^{-1} was determi-

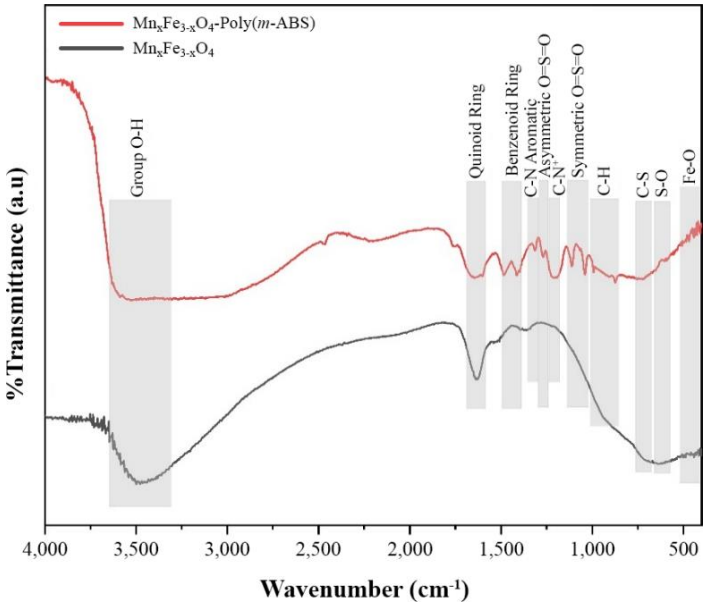

Figure 1. FTIR spectrum of $Mn_xFe_{3-x}O_4$-Poly(*m*-ABS) and $Mn_xFe_{3-x}O_4$.

ned as characteristic of the S-O strain in the sulfonic and C-S aromatic groups [9], [11], [23]–[25]. The absorption peaks at 874 cm^{-1} and 991 cm^{-1} indicated the presence of C-H outside the vibrational plane, indicating the presence of 1, 2, 4, and 1,4 substituted benzene rings, indicating that the monomers in the polymer are head-to-tail is required in the formation of polymer chains [7], [9], [11]. The Fe-O functional group was detected in the vibrational wave number 552 cm^{-1} according to the Fe-O absorption range at 500–750 cm^{-1} [26], [27]. The appearance of asymmetric and symmetrical strains O=S=O, S-O, and C-S strains is the main characteristic of poly(*m*-ABS) which indicates the success of monomer polymerization [11].

3.2. XRD Characterization

The results of the XRD characterization of the $Mn_xFe_{3-x}O_4$-Poly(*m*-ABS) nanocomposite can be seen in Figure 2. The diffraction peaks in the XRD data have been adjusted to the Fe_3O_4 diffraction pattern, which refers to the AMCSD 0007423 database. In the XRD data, it can be observed that several peaks appear at the value of 2θ, *i.e.* 30.23°, 35.56°, 43.24°, 57.12°, and 62.84°, with the hkl planes being (220), (311), (400), (422), (511), and (440), the resulting diffraction peaks indicate that the structure is cubic spinel [28]. The appearance of peaks (111), (620) with low intensity, and (440) showed that the synthesized polymer had its crystal structure, as reported by Shabzendedar *et al.* [12]. The relatively small peak intensity is also possible due to a rigid benzene ring in the polymer chain, which can prevent the formation of a crystal structure [29]. This is also supported by the characteristics of polyaniline, which tends to have the characteristics of amorphous materials [30].

The particle size of the $Mn_xFe_{3-x}O_4$-Poly(*m*-ABS) nanocomposite was analyzed quantitatively using Origin software using the Debye-Scherrer equation (Equation 1).

$$D = \frac{K\,\lambda}{\beta \cos\theta} \tag{1}$$

D is the crystal size, K is a constant, β is the width of half the peak in maximum intensity (FWHM), λ is the wavelength, and θ is the Bragg angle of the highest peak [31]. The measurement results using Equation 1 obtained the particle size of the nanocomposite $Mn_xFe_{3-x}O_4$-Poly(*m*-ABS) ranging from 10.62 nm. This result is not much different from the $Mn_xFe_{3-x}O_4$@PANI composite reported by Sunaryono *et al.* at 8.09 nm [8] and the Fe_3O_4/PANI composite reported by Ismail *et al.* at 14.3 nm, which confirms the nano size of ferrite [32]. Shabzendedar *et al.* also reported that the *m*-aminobenzenesulfonic acid-Fe_3O_4 (NCPABS-Fe_3O_4) composite has a particle size of 48 nm and was applied to polymer solar cells [12]. The nanoscale particle size has been found to be effective for enhancing dye absorption and improving sunlight absorption to increase solar cell efficiency [33], [34].

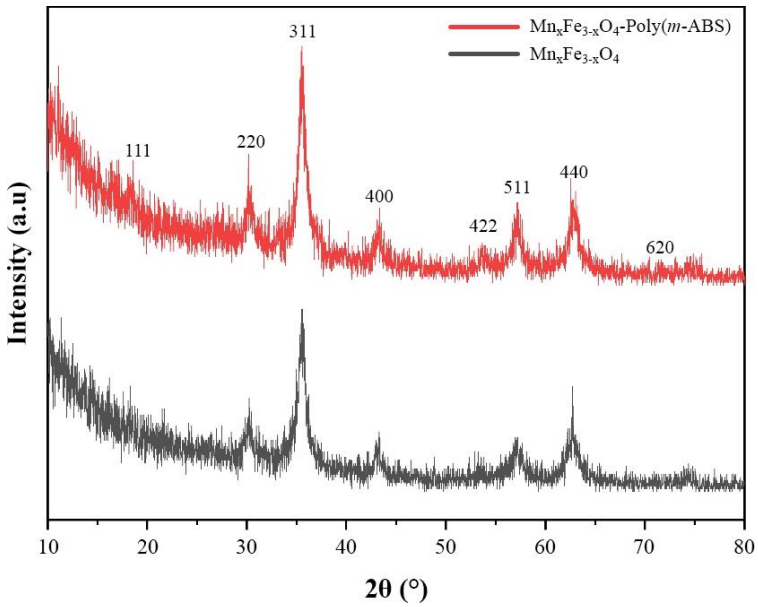

Figure 2. XRD characterization of $Mn_xFe_{3-x}O_4$-Poly(*m*-ABS) and $Mn_xFe_{3-x}O_4$.

3.3. SEM Characterization

The surface morphology of the $Mn_xFe_{3-x}O_4$-Poly(*m*-ABS) nanocomposite was characterized by SEM, which is shown in Figure 3. The results of the SEM image analysis can be seen that circular shapes dominate the shape with varying sizes. The particles experience agglomeration, which causes the appearance of clusters of particles. The appearance of a group of particles can occur due to agglomeration events in the sample. SEM analysis showed an average particle size of 42 nm. The particle size of $Mn_xFe_{3-x}O_4$-Poly(*m*-ABS) nanocomposite corresponds to the core-shell nanocomposite of poly(*m*-ABS acid)-Fe_3O_4 (NCPABS-Fe_3O_4) at 42 nm for solar cell polymers [12] and also Fe_3O_4@PANI composites at 48 nm for solar cell polymers [7] using SEM analysis. From the structural analysis results obtained, the potential of $Mn_xFe_{3-x}O_4$-Poly(*m*-ABS) nanocomposite to be applied as a solar cell polymer material is quite possible, coupled with the nanoscale particle size, which is reported to increase the absorption of sunlight [34]. The particle size obtained from the SEM characterization is much larger than the particle size from the XRD characterization. This is because the SEM characterization only measures the particle's surface, so what is measured is the diameter of the particle cluster [35].

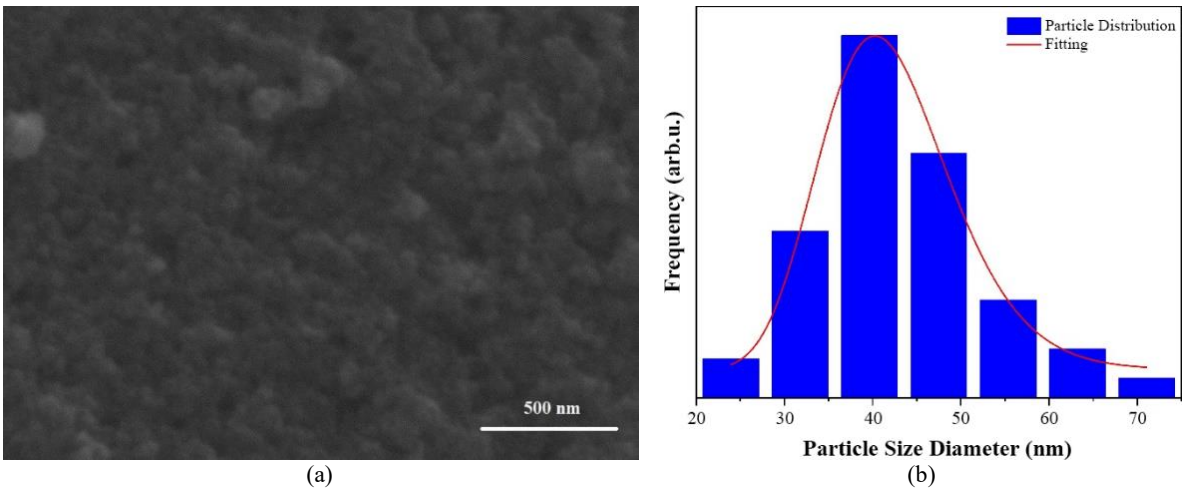

(a) (b)

Figure 3. (a) SEM image of $Mn_xFe_{3-x}O_4$-Poly(*m*-ABS), (b) particle size distribution of $Mn_xFe_{3-x}O_4$-Poly(*m*-ABS) nanocomposites.

4. Conclusion

Synthesis of $Mn_xFe_{3-x}O_4$-Poly(*m*-ABS) nanocomposite based on iron sand has been successfully carried out. The particle size was 10.62 nm with a spinel cubic structure from the XRD characterization. The appearance of peaks with low intensity, *i.e.* (111) and (620), indicates that the synthesized polymer has its crystal structure. The relatively small intensity can be influenced by polyaniline's nature, which tends to be amorphous. Based on the FTIR spectrum, the appearance of asymmetric and symmetrical strains O=S=O, S-O, and C-S strains are the main characteristics of poly(*m*-ABS) which indicate the success of monomer polymerization. SEM analysis shows a particle size of 42 nm, this result is different from XRD results because SEM can only measure the particle's surface, so the resulting size tends to be larger. From the study results of the structure obtained, the $Mn_xFe_{3-x}O_4$-Poly(*m*-ABS) nanocomposite allows it to be applied as an energy conversion material, supported by the nanoscale particle size which is reported to increase the absorption of sunlight.

References

[1] M. Nasrollahzadeh, S. M. Sajadi, M. Sajjadi, and Z. Issaabadi, "applications of nanotechnology in daily life," in *An Introduction to Green Nanotechnology*. London, U.K.: Elseiver, 2019, ch. 4, pp. 113–143.

[2] T. Saragi *et al.*, "Synthesis and properties of iron oxide particles prepared by hidrothermal method," in *IOP Conf. Ser.: Mat. Sci. Eng.*, vol. 196, no. 1, p. 012025, 2017, doi: 10.1088/1757-899X/196/1/012025.

[3] S. Moise *et al.*, "The cellular magnetic response and biocompatibility of biogenic zinc-and cobalt-doped magnetite nanoparticles," *Sci. Rep.*, vol. 7, no. 1, p. 39922, 2017, doi: 10.1038/srep39922.

[4] I. P. T. Indrayana, "Review Fe3O4 dari pasir besi : Sintesis, karakterisasi, dan fungsionalisasi hingga aplikasinya dalam bidang nanoteknologi maju," *Uniera*, vol. 8, no. 2, pp. 65–75, 2019.

[5] A. Eftekhari, L. Li, and Y. Yang, "Polyaniline supercapacitors," *J. Power Sources*, vol. 347, pp. 86–107, 2017, doi: 10.1016/j.jpowsour.2017.02.054.

[6] X. Wang *et al.*, "Bio template synthesis of Fe3O4/Polyaniline for supercapacitor," *J. Energy Storage*, vol. 30, p. 101554, 2020, doi: 10.1016/j.est.2020.101554.

[7] F. Sadegh, A. R. Modarresi-Alam, M. Noroozifar, and K. Kerman, "A facile and green synthesis of superparamagnetic Fe3O4@PANI nanocomposite with a core-shell structure to increase of triplet state population and efficiency of the solar cells," *J. Environ. Chem. Eng.*, vol. 9, no. 1, p. 104942, 2021, doi: 10.1016/j.jece.2020.104942.

[8] Sunaryono, N. M. Chusna, A. Taufiq, N. Mufti, and S. Hidayat, "The influence of alternating magnetic field frequency on magneto-thermal behavior of Mn0.25Fe2.75O4@PANI material," in *IOP Conf. Ser.: Mater. Sci. Eng.*, vol. 515, no. 1, p. 012035, 2019, doi: 10.1088/1757-899X/515/1/012035.

[9] P. Bandyopadhyay *et al.*, "Facile synthesis of novel sulfonated polyaniline functionalized graphene using m-aminobenzene sulfonic acid for asymmetric supercapacitor application," *Chem. Eng. J.*, vol. 308, pp. 1174–1184, 2017, doi: 10.1016/j.cej.2016.10.015.

[10] M. Das, S. S. Bhunia, and S. Roy, "Poly (m-amino benzene sulfonic acid)-based composites on plastic substrates: A simple and cost-effective approach towards low ppm ammonia detection at room temperature and kinetic analysis," *Synth. Met.*, vol. 248, pp. 1–13, 2019, doi: 10.1016/j.synthmet.2018.12.019.

[11] A. R. Modarresi-Alam *et al.*, "A solid-state synthesis, mechanism, and characterization of high molecular weight poly (3-aminobenzenesulfonic acid) with FeCl3.6H2O as a binary oxidant and dopant," *J. Polym. Res.*, vol. 26, no. 1, pp. 1–16, 2019, doi: 10.1007/s10965-018-1674-4.

[12] S. Shabzendedar, A. R. Modarresi-Alam, M. Noroozifar, and K. Kerman, "Core-shell nanocomposite of superparamagnetic Fe3O4 nanoparticles with poly(m-aminobenzenesulfonic acid) for polymer solar cells," *Org. Electron.*, vol. 77, p. 105462, 2019, doi: 10.1016/j.orgel.2019.105462.

[13] Sunaryono *et al.*, "Magneto-thermal behavior of MnxFe3-xO4-PVA/PVP magnetic hydrogel and its potential application," in *AIP Conf. Proc.*, vol. 2228, no. 1, p. 030018, 2020, doi: 10.1063/5.0000890.

[14] S. Sumardiono *et al.*, "Physicochemical properties of sago ozone oxidation: The effect of reaction time, acidity, and concentration of starch," *Foods*, vol. 10, no. 6, p. 1309, 2021, doi:

10.3390/foods10061309.
[15] T. Miao, E. J. Miller, C. McKenzie, and R. A. Oldinski, "Physically crosslinked polyvinyl alcohol and gelatin interpenetrating polymer network theta-gels for cartilage regeneration," *J. Mat. Chem. B*, vol. 3, no. 48, pp. 9242–9249, 2015, doi: 10.1039/C5TB00989H.
[16] Y. Yan *et al.*, "Carbon nanotube catalysts: Recent advances in synthesis, characterization and applications," *Chem. Soc. Rev.*, vol. 44, no. 10, pp. 3295–3346, 2015, doi: 10.1039/C4CS00492B.
[17] J. Gao *et al.*, "Bifacial quasi-solid-state dye-sensitized solar cells with Poly (vinyl pyrrolidone)/polyaniline transparent counter electrode," *Nano Energy*, vol. 26, pp. 123–130, 2016, doi: 10.1016/j.nanoen.2016.05.010.
[18] J. Tang *et al.*, "Synthesis and electromagnetic properties of PANI/PVP/CIP core-shell composites," *Mater. Sci. Eng.: B*, vol. 186, pp. 26–32, 2014, doi: 10.1016/j.mseb.2014.02.003.
[19] A. R. Modarresi-Alam *et al.*, "The first report of polymerization and characterization of aniline bearing chiral alkyl group on ring via covalent bond; Poly[(±)-2-(sec-butyl)aniline]," *J. Mol. Struct.*, vol. 1083, pp. 17–26, 2015, doi: 10.1016/j.molstruc.2014.11.003.
[20] F. Movahedifar and A. R. Modarresi-Alam, "The effect of initiators and oxidants on the morphology of poly [(±)-2-(sec-butyl) aniline] a chiral bulky substituted polyaniline derivative," *Polym. Adv. Technol.*, vol. 27, no. 1, pp. 131–139, 2016, doi: 10.1002/pat.3614.
[21] A. Farrokhzadeh and A. R. Modarresi-Alam, "Complete doping in solid-state by silica-supported perchloric acid as dopant solid acid: Synthesis and characterization of the novel chiral composite of poly [(±)-2-(sec-butyl) aniline]," *J. Solid State Chem.*, vol. 237, pp. 258–268, 2016, doi: 10.1016/j.jssc.2016.02.032.
[22] H. B. Koosheh and A. R. Modarresi-Alam, "Solid-state synthesis of a new core-shell nanocomposite of polyaniline and silica via oxidation of aniline hydrochloride by FeCl3.6H2O," *Polym. Adv. Technol.*, vol. 27, no. 8, pp. 1038–1049, 2016, doi: 10.1002/pat.3766.
[23] P. Bandyopadhyay *et al.*, "Facile synthesis of novel sulfonated polyaniline functionalized graphene using m-aminobenzene sulfonic acid for asymmetric supercapacitor application," *Chem. Eng. J.*, vol. 308, pp. 1174–1184, 2017, doi: 10.1016/j.cej.2016.10.015.
[24] X. Zheng *et al.*, "Self-powered electrochemistry for the oxidation of organic molecules by a cross-linked triboelectric nanogenerator," *Adv. Mat.*, vol. 28, no. 26, pp. 5188–5194, 2016, doi: 10.1002/adma.201600133.
[25] S. I. Shoda, H. Uyama, J. I. Kadokawa, S. Kimura, and S. Kobayashi, "Enzymes as green catalysts for precision macromolecular synthesis," *Chem. Rev.*, vol. 116, no. 4, pp. 2307–2413, 2016, doi: 10.1021/acs.chemrev.5b00472.
[26] A. S. Prasad, "Iron oxide nanoparticles synthesized by controlled bio-precipitation using leaf extract of Garlic Vine (*Mansoa alliacea*)," *Mater. Sci. Semicond. Process.*, vol. 53, pp. 79–83, 2016, doi: 10.1016/j.mssp.2016.06.009.
[27] A. A. Alqadami *et al.*, "Synthesis and characterization of Fe3O4@TSC nanocomposite: Highly efficient removal of toxic metal ions from aqueous medium," *RSC Adv.*, vol. 6, no. 27, pp. 22679–22689, 2016, doi: 10.1039/C5RA27525C.
[28] Sunaryono *et al.*, "Contributions of TMAH surfactant on hierarchical structures of PVA/Fe3O4–TMAH ferrogels by using SAXS instrument," *J. Inorg. Organomet. Polym. Mater.*, vol. 28, no. 6, pp. 2206–2212, 2018, doi: 10.1007/s10904-018-0939-z.
[29] G. Ćirić-Marjanović, "Recent advances in polyaniline research: Polymerization mechanisms, structural aspects, properties and applications," *Synt. Met.*, vol. 177, pp. 1–47, 2013, doi: 10.1016/j.synthmet.2013.06.004.
[30] S. T. U. I. Subadra *et al.*, "Preparation and characterization of magnetite nanoparticles combined with polyaniline and activated carbon," in *IOP Conf. Ser.: Earth Environ. Sci.*, vol. 276, no. 1, 2019, doi: 10.1088/1755-1315/276/1/012041.
[31] A. Taufiq *et al.*, "Preparation of superparamagnetic Zn0.5Mn0.5Fe2O4 particle by coprecipitation-sonochemical method for radar absorbing material," in *IOP Conf. Ser.: Mater. Sci. Eng.*, vol. 202, no. 1, p. 012024, 2017, doi: 10.1088/1757-899X/202/1/012024.
[32] M. M. Ismail, S. N. Rafeeq, J. Sulaiman, and A. Mandal, "Electromagnetic interference shielding and microwave absorption properties of cobalt ferrite CoFe2O4/polyaniline composite," *Appl. Phys. A*, vol. 124, no. 5, pp. 1–12, 2018, doi: 10.1007/s00339-018-1808-x.

[33] S. Wahyuningsih, A. H. Ramelan, A. N. Firdaus, and R. E. Cahyono, "Preparation composite TiO2 anatase with polydimetilsiloxane and polytetrafluoroethylene for self cleaning on glass substrate," in *IOP Conf. Ser.: Mat. Sci. Eng.*, vol. 858, no. 1, p. 012020, 2020, doi: 10.1088/1757-899X/858/1/012020.

[34] Y. Septriani and M. Muldarisnur, "Kontrol ukuran nanopartikel perak dengan variasi konsentrasi ekstrak kulit buah manggis," *J. Fis. Unand,* vol. 11, no. 1, pp. 68–74, 2022, doi: 10.25077/jfu.11.1.68-74.2022.

[35] A. Taufiq *et al.*, "Exploring magnetic properties and antimicrobial activities of Co0.4Fe2.6O4ferrofluids using olive oil as dispersant agent," in *AIP Conf. Proc.*, vol. 2251, no. 1, p. 030002, 2020, doi: 10.1063/5.0015623.